Fibers and Polymers 2017, Vol.18, No.5, 915-921
DOI 10.1007/s12221-017-6922-4

ISSN 1229-9197 (print version)
ISSN 1875-0052 (electronic version)

Properties of Flame-retardant Cellulose Fibers with Ionic Liquid

Yang Liu, Zeming Jiang, Jiaojiao Miao, Yongqi Yu, and Liping Zhang*

MOE Engineering Research Center of Forestry Biomass Materials and Bioenergy, College of Materials Science and Technology, Beijing Forestry University, Beijing 100083, People's Republic of China

(Received September 20, 2016; Revised November 7, 2016; Accepted February 18, 2017)

Abstract: Flame-retardant cellulose fibers were prepared by dissolving cellulose in tetrabutylammonium acetate and dimethyl sulfoxide, and blending with amino silicone oil (ASO). The ASO was used as a novel fabric softener and flame retardant for cellulose fibers. Fourier-transform infrared spectroscopy showed that blending with ASO did not adversely affect the cellulose fibers. The flame retardancy of the cellulose fibers blended with ASO was determined based on the limiting oxygen index (LOI). Cellulose fibers blended with 8 wt% (add-on) ASO gave the best flame retardancy, with an LOI of 28, which was higher than that of the virgin fibers. The thermal properties of the flame-retardant cellulose fibers were investigated using differential scanning calorimetry and thermogravimetric analysis. The results showed that ASO prevented degradation of the cellulose fibers, hindered the formation of volatile species, and favored char formation. The mechanical properties of the flame-retardant cellulose fibers were better than those of virgin cellulose fibers.

Keywords: Flame retardant, Fabric softener, Cellulose fiber, Tetrabutylammonium acetate (TBAA), Thermal properties

Introduction

Cellulose is the most abundant renewable organic material produced in the biosphere. It is a linear homopolymer composed of D-anhydroglucopyranose units, which are linked by β-(1-4)-gylcosidic bonds [1]. Cellulose fibers have good mechanical properties, with a maximum macroscopic Young's modulus (138 GPa) higher than those of aluminum (69 GPa) and glass fibers (69 GPa) [2]. Cellulose fibers have a number of other advantages over conventional reinforcing materials such as thermal recyclability by combustion, biodegradability, and hydrophilicity. Another attraction is that its low density results in good specific mechanical properties [2-4]. Because of these properties, cellulose is an ideal high-performance biocomposite. However, cellulose fibers also have disadvantages such as flammability, and these restrict their industrial applications. It is necessary to reduce the flammability of cellulose fibers for safety reasons [5]. This can be achieved using flame retardants, which act through various mechanisms.

There are many ways to improve the flame-retardant properties of fabrics, such as blending, coating, finishing, and so on in previously studies [6-9]. Flame retardancy is imparted to cellulose fibers by addition of a flame retardant to the cellulose solution. The additive must meet several requirements, *e.g.*, good compatibility with the cellulose solution and an appropriate particle size, to avoid spinneret clogging [10,11]. Halogen-containing compounds are excellent flame retardants, but their use is restricted because they generate toxic and corrosive gases during combustion [12]. Non-halogen flame retardants containing phosphorus, nitrogen, or silicon, which are less toxic than halogen-containing retardants, are widely used as flame retardants for textiles [3,13,14]. Application of inorganic nano-particles on textiles would also be a good alternative to conventional materials and consequently, they can open up a new opportunity for multi-functional modification of fibers, such as nano-ZrO_2, graphene, and so on [15-17]. Silicones impart desired mechanical properties such as softness, bounciness, and anti-wrinkle properties to fabrics and related materials [18,19]; the most widely used silicone materials are poly(dimethylsiloxane)s. Because of their inorganic-organic structure and the flexibility of silicone bonds, silicones have properties such as thermal oxidative stability, low-temperature flowability, small viscosity changes with changes in temperature, high compressibility, low surface tension, hydrophobicity, and good electrical properties with a low fire risk. Many silicone materials are effective at very low concentrations [20,21].

Amino silicones show superior softening and mechanical properties, possibly because of their excellent film-forming ability and morphology [22]. Figure 1 shows the mechanism of the reaction between cellulose and amino silicone oil (ASO). The figure also shows that cellulose and the ASO blend well.

Ionic liquids are attracting increasing attention as a new class of solvents [23] because of their high thermostability, low viscosity, non-volatility, and ease of recycling, so ionic liquids can also be used in many fields. In other studies, ionic liquids can act as a medium or a cross-linking agent for the activation reaction, extract the lignin in cellulose and so on [24,25]. We previously studied the behavior of cellulose dissolved in a mixture of tetrabutylammonium acetate (TBAA) and dimethyl sulfoxide (DMSO) [26]. To the best of our knowledge, there are no reports in the literature of studies of the flame-retardant properties of cellulose fibers prepared in a TBAA-DMSO solution with ASO as a fire-retardant additive. In this study, a novel fabric softener and

*Corresponding author: zhanglp418@163.com

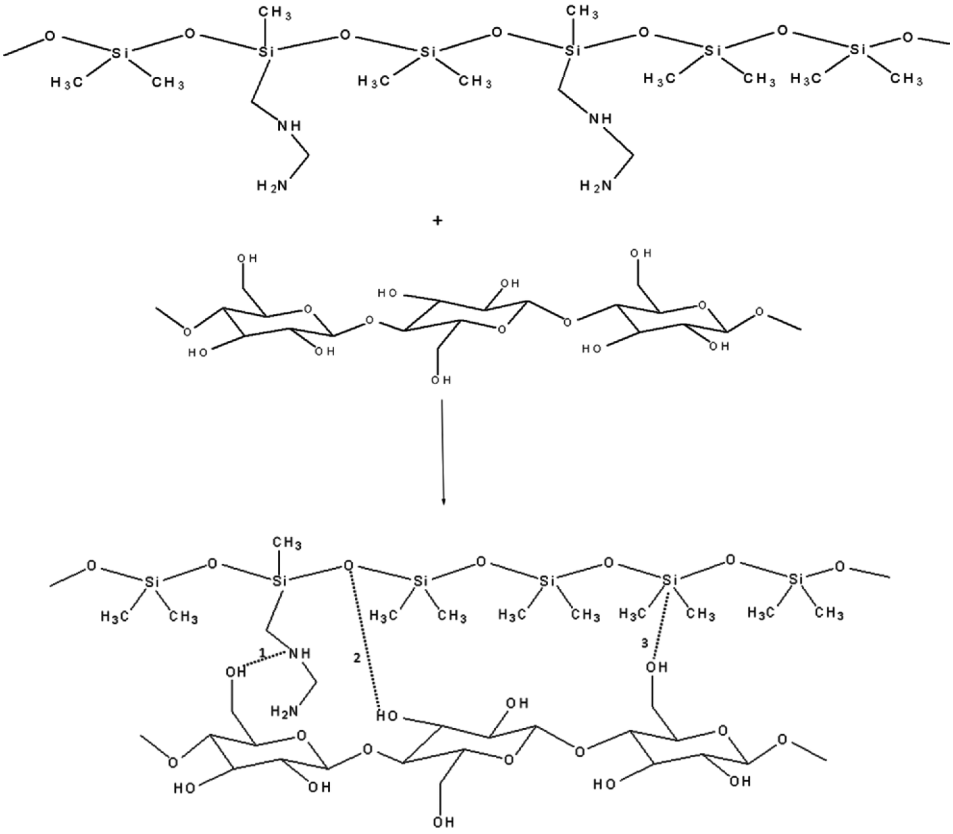

Figure 1. Mechanism of reaction between cellulose and ASO; (1) ionic interaction, (2) hydrogen bond, and (3) covalent ether bond between cellulose and amino silicone molecules.

flame retardant, *i.e.*, ASO, was synthesized and used in the preparation of flame-retardant cellulose fibers via a blending wet-spinning method. The structure of the blended fibers was examined using fourier-transform infrared (FTIR) spectroscopy. The flame retardancy was evaluated based on the limiting oxygen index (LOI), and the thermal stability and mechanical properties of the flame-retardant cellulose fibers were investigated using differential scanning calorimetry (DSC) and thermogravimetric analysis (TGA).

Experimental

Materials

Cellulose pulp (degree of polymerization 900) was supplied by the Rizhao Senbo Pulp Paper Co., Ltd., China. ASO (R-80) was purchased from the Shanghai Juanrui Chemical Company. TBAA (purity >90 %) was obtained from TCI Chemicals. All other reagents were purchased from commercial sources in China and were analytical grade.

Solution Preparation

Cellulose pulp (1.6 g) was added to a TBAA/DMSO (mass ratio 2:8) solvent mixture (20 g), and the dispersion was stirred at 65 °C for 1 h. The cellulose pulp was dried under vacuum in an oven at 80 °C to remove water. ASO (0, 1.0, 1.2, 1.4, or 1.6 g) was added dropwise with stirring and

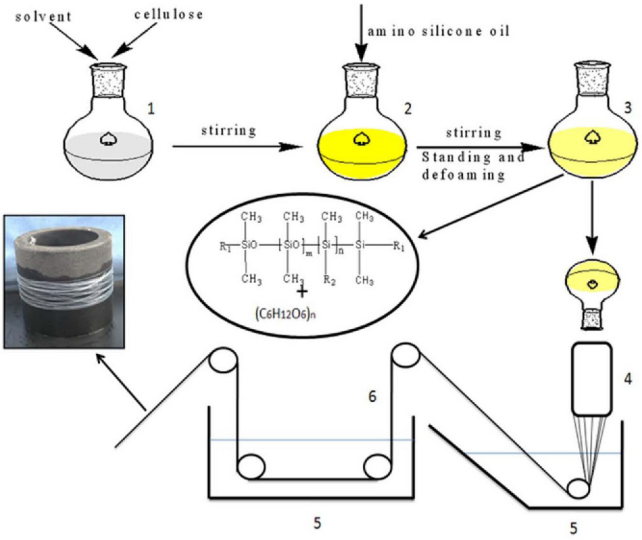

Figure 2. Protocol for preparation of blended cellulose fibers; (1-3) solution preparation, (4) spinneret, (5) coagulating bath, and (6) stretching machine.

the mixture was stirred at 65 °C for 2 h. A vacuum pump was used to remove air bubbles from the solution at 70 °C for 1 h.

Spinning Trials

A laboratory-scale dry-jet wet-spinning apparatus consisting of a micro-syringe propulsion device, a glass syringe (inner diameter, 10 mm *Φ*) with a needle (length, 32 mm; inner diameter, 0.37 mm *Φ*) as a spinneret, a spinning bath and a take-up device was constructed in our laboratory. The extrusion speed was 0.6 m*l*/min; the temperatures of the spinning dope and the coagulating bath were 65 °C and 25 °C, respectively.

Characterization

The chemical structure of the fibers was investigated using FTIR spectroscopy (VERTES TOV, Bruker, Germany). The scanning range was 4000-450 cm^{-1}.

The morphology (surface and cross section) of the blended fibers spun from cellulose was examined using a scanning electron microscope (SEM; S-3400 N, Hitachi). The fibers were frozen in liquid nitrogen, immediately snapped, and then vacuum dried. The samples were sputtered with gold before being observed and photographed.

The LOI was determined (GB/T2406.2-2009) using an HC-2 oxygen index meter (Jiangning Analytical Instrument Company, China). The dimensions of the specimens used for the tests were 120×50 mm^2.

TG experiments were performed using an STA 449F3 instrument (Netzsch, Germany). The sample weights were 5-8 mg. TGA was performed in a nitrogen flow at 50 °C to 600 °C at a heating rate of 10 °C/min.

DSC was performed using a Mettler Toledo DSC 821 analyzer, from 25 °C to 350 °C at a heating rate of 10 °C/min in a continuous air flow.

The mechanical properties were investigated using a strong pull machine (ZB-WL300) at 20 °C. The results for 10 different samples were averaged. The gauge length was 10 mm, the test speed was 1.0 mm/min, and the preload was 1.0 cN/dtex.

Results and Discussion

Characterization and Measurements

FTIR spectroscopy has been widely used to study the interactions in polymer blends [27-31]. FTIR spectra of the cellulose/ASO blend fibers are shown in Figure 3. The spectra of all the samples have a weak hydroxyl stretching absorption peak at 3429 cm^{-1}. When the added amount of was ASO increased, absorption peaks from C-N, C-Si, and N-H appeared at 1026, 802, and 669 cm^{-1}, respectively; the peak intensities increased with increasing amount of ASO. Peaks at 2901 cm^{-1}, ascribed to aliphatic -CH_2 stretching, and 1636 cm^{-1}, assigned to amine C-N bond vibrations, also appeared. The peak at 1250 cm^{-1} was assigned to C-Si deformation vibrations. These findings indicate that chemical reactions occurred between cellulose and ASO during spinning.

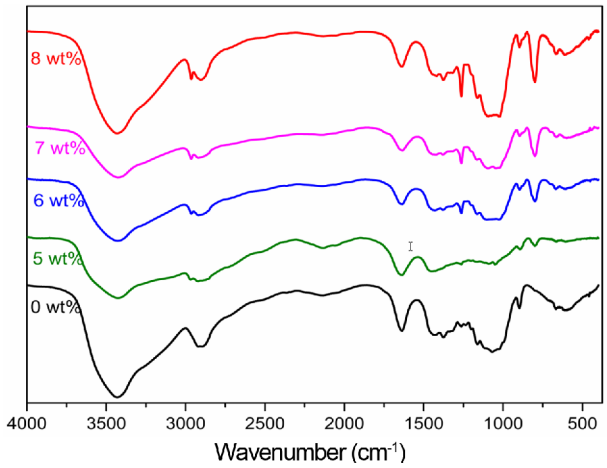

Figure 3. FTIR spectra of cellulose and cellulose/ASO fibers.

The morphologies of the blend fibers were investigated using SEM; Figure 4(a)-(e) show images of the surfaces and cross sections of cellulose fibers containing 0, 5, 6, 7, and 8 wt% ASO. The SEM images show that the virgin cellulose fibers (0 wt% ASO) were tidy, smooth, and uniform. However, the surfaces and cross sections of cellulose blended with the flame retardant were rough and uneven with clear grooves and cracks. Figure 4 shows that the morphology of the blend fibers improved with increasing ASO content. When the ASO content was 8 wt%, the surface and cross section images of the blend fibers showed no obvious grooves and cracks.

LOI

Figure 5 and Table 1 (inset in Figure 5) show the LOI values of blend cellulose fibers with various ASO contents. The data show that the LOI of the cellulose fibers containing no ASM was 19; the LOIs of the cellulose fibers containing 5, 6, 7, and 8 wt% ASO were 21, 23, 25, and 28, respectively, the cellulose fiber LOI gradually increased with increasing ASO content. The cellulose fiber LOI reached 28, achieving the general requirement for flame-retardant standard, when the ASO content was 8 wt%. The LOI values of other flame retardant fibers are 28 or over 28 in other previously studies [32,33]. This is because ASO decomposes during thermal degradation and produces incombustible gases, which reduce the concentration of flammable gases and form char layers. ASO also produces silicon and nitrogen, which act as a physical barrier and protect the cellulose fibers from heat and oxygen transfer. The flame-retarding mechanism involves migration of the flame retardant to the material surface and production of a siliceous char layer during combustion [34]. The Si-N

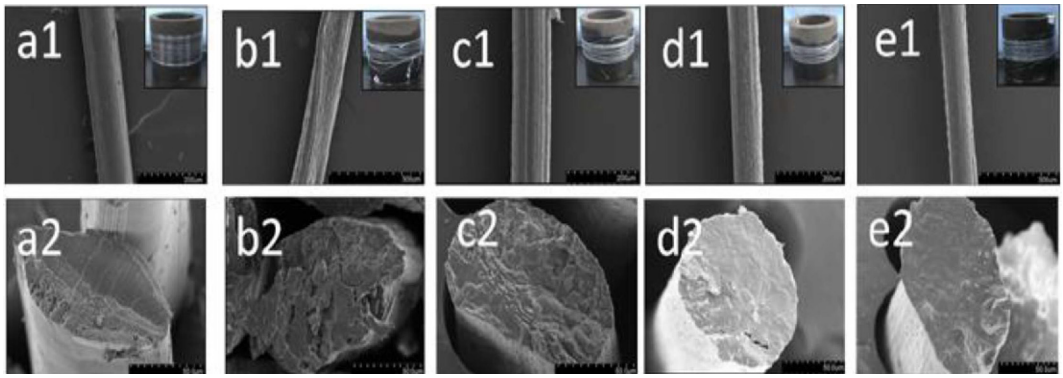

Figure 4. SEM images of cellulose fibers with various ASO contents: (a1-e1: the images of the surfaces of the blended cellulose fibers; a2-e2: the images of the cross sections of the blended cellulose fibers) (a1, a2) 0 wt%, (b1, b2) 5 wt%, (c1, c2) 6 wt%, (d1, d2) 7 wt%, and (e1, e2) 8 wt%.

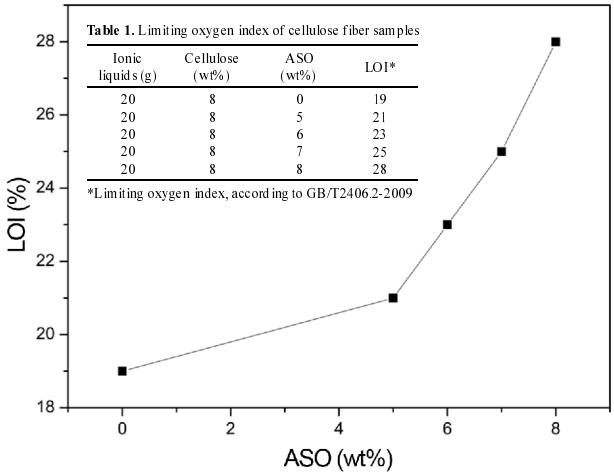

Table 1. Limiting oxygen index of cellulose fiber samples

Ionic liquids (g)	Cellulose (wt%)	ASO (wt%)	LOI*
20	8	0	19
20	8	5	21
20	8	6	23
20	8	7	25
20	8	8	28

*Limiting oxygen index, according to GB/T2406.2-2009

Figure 5. LOIs of cellulose fibers with various ASO contents.

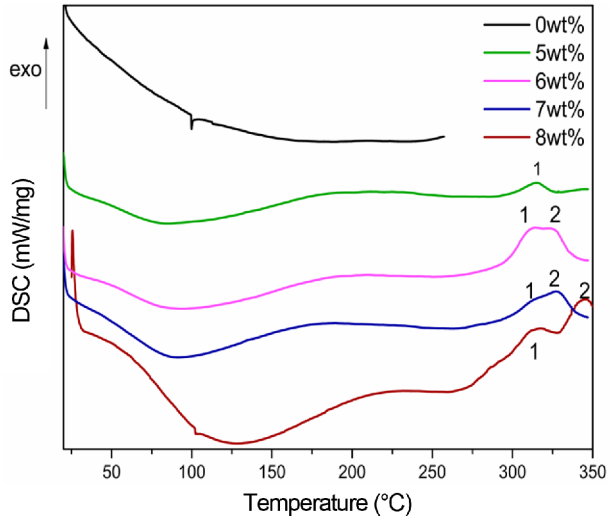

Figure 6. DSC curves of cellulose fibers with various ASO contents.

system is of great value because of its inherent high flame-retarding efficiency and good thermal durability at elevated temperatures.

Thermal Analysis

The DSC curves of the cellulose fiber samples in a nitrogen atmosphere are shown in Figure 6. The low-temperature and higher-temperature exothermic peaks at 250-350 °C in the DSC curves are labeled 1 and 2, respectively, and the temperatures are listed in Table 2. The sample containing 0 wt% ASO was virgin cellulose fibers. There was no obvious exothermic peak in the DSC curve of the virgin cellulose fibers. In the DSC curves of the cellulose fiber samples containing 5, 6, 7, and 8 wt% ASO, the exothermic peaks 1 appeared at 315.9, 312.3, 312.8, and 315.0 °C, respectively. These results show that ASO addition caused the appearance of an exothermic peak, *i.e.*, the cellulose had reacted with the ASO. The DSC curves of the cellulose fibers containing 6, 7, and 8 wt% ASO showed exothermic peaks 2 at 326.6 °C, 328.0 °C, and 345.3 °C, respectively, but

Table 2. Exothermic peak temperatures of cellulose fiber samples

Content of ASM (wt%)	Main peak temperatures (°C)	
	1	2
0	-	-
5	315.9	-
6	312.3	326.6
7	312.8	328.0
8	315.0	345.3

the DSC curve of the cellulose fibers containing 5 wt% ASO did not show a corresponding peak. The values reported in the literature for the exothermic peaks 1 and 2 of virgin cellulose fibers are 373.5 °C and 498.6 °C, respectively [5]. These results show that ASO addition can change the cellulose fiber decomposition temperature by up to 50 °C. The exothermic peak 1 at about 315 °C for the blend cellulose fibers suggests that exothermic pyrolysis of ASO began at that temperature. This reaction results in the

cellulose decomposition temperature decreasing from that of virgin cellulose, which degrades to laevoglucose at 373.5 °C, to 315 °C. The changes in the exothermic peak temperatures indicate that ASO promoted cellulose decomposition at a lower temperature. Silica, which is strongly dehydrating, is a possible ASO degradation product. It is also an efficient flame retardant for cellulose fibers because a silica coating on cellulose favors char formation [35]. ASO addition can therefore promote cellulose charring and reduce CO production. The char produced from cellulose and silica from the decomposition of ASO could effectively isolate oxygen and prevent continuous combustion, providing a condensation-phase flame-retardant effect. Nitrogen and NO_2 released from ASO combustion, which are inert gases and hard to burn, dilute the oxygen present. This is the gas-phase flame-retardant effect.

TGA curves of cellulose fibers containing various amounts of ASO are shown in Figure 7 and the corresponding parameters are shown in Table 3. The main weight-loss stage (250-500 °C) for the cellulose fiber samples indicated primary decomposition and charring of cellulose. At this stage, the temperatures for the maximum weight-loss rate and termination of decomposition were 329.8 °C and 370.8 °C, respectively, and the weight loss for virgin cellulose fibers

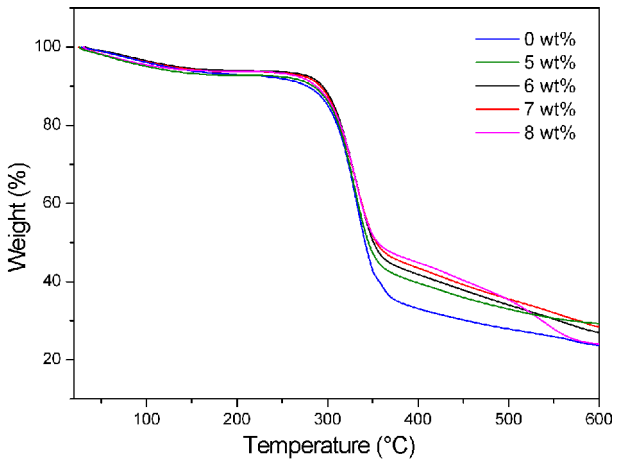

Figure 7. TGA curves of cellulose fibers with various ASO contents.

Table 3. TGA data for cellulose fiber samples

Contents of ASM (wt%)	Main stage			Residual mass (%)
	Temperature of maximum weight loss (°C)	Decomposition end temperature (°C)	Weight loss percentage (%)	
0	329.8	370.8	52.6	23.60
5	328.6	365.2	47.2	29.30
6	327.8	362.0	45.5	27.00
7	325.7	361.0	43.5	28.50
8	320.0	364.4	42.8	24.05

was 52.6 %. Many researchers have reported that cellulose fiber degradation in nitrogen involves two competitive routes: cellulose depolymerization, resulting in production of volatile species (*e.g.*, laevoglucose), and dehydration, leading to formation of a thermally stable carbonaceous structure (char) [36]. The temperature for the maximum weight-loss rate for cellulose fibers containing 5, 6, 7, and 8 wt% ASO were 328.6 °C, 327.8 °C, 325.7 °C, and 320.0 °C, respectively. The temperature at which the weight-loss rate for ASO-modified cellulose fibers was maximum was 5-10 °C lower than that for virgin cellulose fibers; the temperature also decreased with increasing ASO content. The temperature at which decomposition ended and the percentage weight loss for cellulose blended fibers were lower than those for virgin cellulose fibers. These results indicate that the addition of ASO reduced the maximum weight-loss temperature and the temperature at which decomposition ended, promoted cellulose dehydration to laevoglucose, and increased char formation.

Figure 7 and the corresponding data in Table 3 show that further decomposition and charring of cellulose occurred in the final stage (350-600 °C). The percentage weight loss of virgin cellulose was higher than those of the modified samples. The residual mass of the control sample was lower than those of the modified samples. This is because formation of flammable small-molecule products derived from further decomposition of virgin cellulose fibers could enable cellulose fiber combustion to continue, leading to further weight loss. The TGA results indicate that treatment of cellulose fibers with ASO lowers the decomposition temperature and enhances char formation during pyrolysis.

Physico-mechanical Properties

The physico-mechanical properties of the cellulose/ASO blend fibers are shown in Figure 8. The tensile strength, elongation at break, and elastic modulus increased with increasing ASO content; therefore, ASO is an important phase in the blend and affects the physico-mechanical

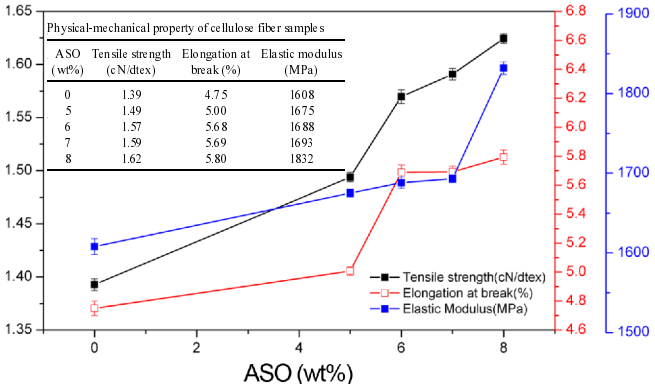

Figure 8. Physico-mechanical properties of cellulose fibers with various ASO contents.

strength. The elastic modulus of the cellulose fibers containing no ASO was 1608 MPa, and those of the cellulose fibers containing 5 wt%, 6 wt%, 7 wt%, and 8 wt% ASO were 1675 MPa, 1688 MPa, 1693 MPa, and 1832 MPa, respectively. The elastic modulus increased because addition of a soft chain polymer such as ASO hardens the cellulose fibers, in Figure 1 and the FT-IR can also indicated that the hydrogen bond were formed between cellulose and amino silicone oil. So, the mechanical properties of the composites were greatly improved by blending ASO.

Conclusion

The use of ASO as an effective novel fabric softener and flame retardant for cellulose fibers was investigated. The results show that the blended cellulose fibers were cylindrical and covered with an oily substance. The LOI of cellulose fibers blended with 8 wt% (add-on) ASO was 28, which is higher than that of virgin cellulose fibers. The morphology of the blend fibers shows that the cellulose and ASO were well blended. DSC and TGA showed that ASO addition lowered the decomposition temperature of cellulose fibers and enhanced char formation during pyrolysis. The silica layer formed by ASO decomposition acted as a thermal insulator, shifting the temperature at which cellulose starts to degrade to higher values. Silica also served as an oxygen barrier, as shown by the significant shifts to higher temperatures of the exothermic peaks (attributed to oxygen combustion). The mechanical properties of the blended cellulose fibers also improved with increasing ASO content. The results suggest that ASO is a good flame retardant and is suitable for use with cellulose fibers. Due to the blended fibers of good flame-retardant properties and mechanical properties, this fiber can be widely used in fire-resistant clothing, fire-retardant wallpaper and more textile field.

Acknowledgements

The authors are grateful for support from the Specialized Research Fund for the Forestry Public Welfare Industry (201504602-2).

References

1. K. Mundsinger, A. Muller, R. Beyer, F. Hermanutz, and M. R. Buchmeiser, *Carbohydr. Polym.*, **131**, 34 (2015).
2. S. J. Eichhorn, A. Dufresne, M. Aranguren, N. E. Marcovich, J. R. Capadona, S. J. Rowan, C. Weder, W. Thielemans, M. Roman, S. Renneckar, W. Gindl, S. Veigel, J. Keckes, H. Yano, K. Abe, M. Nogi, A. N. Nakagaito, A. Mangalam, J. Simonsen, A. S. Benight, A. Bismarck, L. A. Berglund, and T. Peijs, *J. Mater. Sci.*, **45**, 1 (2009).
3. S. Hribernik, M. S. Smole, K. S. Kleinschek, M. Bele, J. Jamnik, and M. Gaberscek, *Polym. Degrad. Stabil.,* **92**, 1957 (2007).
4. I. Siró and D. Plackett, *Cellulose*, **17**, 459 (2010).
5. Y. He, Y. Chen, Q. Zheng, J. Zheng, and S. Chen, *Fiber. Polym.*, **16**, 1005 (2015).
6. M. Parvinzadeh Gashti, R. Rashidian, A. Almasian, and A. Badakhshan Zohouri, *Pigment. Resin. Technol.*, **42**, 175 (2013).
7. M. P. Gashti and M. P. Gashti, *J. Dispersion Sci. Technol.*, **34**, 853 (2013).
8. M. Parvinzadeh Gashti and A. Almasian, *Compos. Pt. B-Eng.*, **52**, 340 (2013).
9. M. Arca, X. Feng, A. J. C. Ladd, and J. E. Butler, *RSC Adv.*, **4**, 1083 (2014).
10. M. Lewin and S. B. Sello, "Handbook of Fiber Science and Technology: Volume II. Chemical Processing of Fibers and Fabrics. Functional Finishes. Part B", CRC Press, 1984.
11. W. D. Schindler and P. J. Hauser, "Chemical Finishing of Textiles", Elsevier, 2004.
12. K. Xie, A. Gao, and Y. Zhang, *Carbohydr. Polym.*, **98**, 706 (2013).
13. S. Gaan and G. Sun, *Polym. Degrad. Stabil.*, **92**, 968 (2007).
14. E. D. Weil and S. V. Levchik, *J. Fire. Sci.*, **26**, 243 (2008).
15. M. Parvinzadeh Gashti and A. Almasian, *Compos. Pt. B-Eng.*, **45**, 282 (2013).
16. M. Parvinzadeh Gashti, A. Almasian, and M. Parvinzadeh Gashti, *Sens. Actuator A-Phys.*, **187**, 1 (2012).
17. Z. Nooralian, M. Parvinzadeh Gashti, and I. Ebrahimi, *RSC Adv.*, **6**, 23288 (2016).
18. W. Noll, "Chemistry and Technology of Silicones", Elsevier, 2012.
19. A. Qiufeng, W. Qianjin, L. Linsheng, and H. Liangxian, *Text. Res. J.*, **79**, 89 (2009).
20. S. J. Clarson and J. A. Semlyen, "Siloxane Polymers", pp.193-215, Prentice Hall, 1993.
21. M. M. Joyner, *Text. Chem. Color.*, **18**, 34 (1986).
22. A. Bereck, B. Weber, and D. Riegel, *Textilveredlung*, **32**, 135 (1997).
23. P. Wasserscheid and W. Thomas, "Ionic Liquids in Synthesis", Vol. 1, Weinheim: Wiley-Vch, 2008.
24. H. Sun, J. Miao, Y. Yu, and L. Zhang, *Appl. Phys. A*, **119**, 539 (2015).
25. J. Miao, H. Sun, Y. Yu, X. Song, and L. Zhang, *RSC Adv.*, **4**, 36721 (2014).
26. J. Miao, Y. Yu, Z. Jiang, and L. Zhang, *Cellulose*, **23**, 1209 (2016).
27. S. Shang, L. Zhu, W. Chen, L. Yi, D. Qi, and L. Yang, *Fiber. Polym.*, **10**, 807 (2010).
28. T. Lü, G. Shan, and S. Shang, *J. Appl. Polym. Sci.*, **118**, 2572 (2010).
29. T. Lü, G. Shan, and S. Shang, *J. Appl. Polym. Sci.*, **122**, 1121 (2011).
30. H. Huang, J. Wu, X. Lin, L. Li, S. Shang, M. C. Yuen, and G. Yan, *Carbohydr. Polym.*, **95**, 72 (2013).

31. Y. Yao, E. Zhang, X. Xia, J. Yu, K. Wu, Y. Zhang, and H. Wang, *Cellulose*, **22**, 625 (2014).
32. J. Alongi, Z. Han, and S. Bourbigot, *Prog. Polym. Sci.*, **51**, 28 (2015).
33. J. Zhang, Z. Liu, Q. Kong, C. Zhang, S. Pang, L. Yue, X. Wang, J. Yao, and G. Cui, *ACS Appl. Mater. Interfaces*, **5**, 128 (2013).
34. J. Vasiljević, S. Hadžić, I. Jerman, L. Černe, B. Tomšič, J. Medved, M. Godec, B. Orel, and B. Simončič, *Polym. Degrad. Stabil.*, **98**, 2602 (2013).
35. J. Alongi, M. Ciobanu, and G. Malucelli, *Cellulose*, **18**, 167 (2010).
36. J. Alongi, G. Camino, and G. Malucelli, *Carbohydr. Polym.*, **92**, 1327 (2013).